Volume 1 | Number 1 | Jan 2013 | Pages 1–100

ChemComm

Chemical Communications
www.rsc.org/chemcomm

ROYAL SOCIETY OF CHEMISTRY

ROYAL SOCIETY OF CHEMISTRY

www.rsc.org/chemcomm

ChemComm

Communication

Polymorphism of metal-organic frameworks: Direct comparison of structures and theoretical N$_2$-uptake of topological *pto*- and *tbo*-isomers

Nianyong Zhu,[a] **Matthew J. Lennox,**[b] **Tina Düren,**[b] **and Wolfgang Schmitt*[a]**

The syntheses, calculated surface areas and N$_2$ uptakes of two highly augmented {Cu}$_2$ 'paddlewheel'-based MOFs provide a direct comparison of *tbo* or *pto* framework polymorphs with identical composition.

10 The exceptional interest in metal-organic frameworks (MOFs) is a result of their advantageous characteristics, which include high porosity, structural and constitutional diversity and amenability to modification for targeting purposes.[1,2] MOFs are regarded as key compounds related to energy storage and conversion,[3] as their 15 attributes in combination with un-precedented surface areas make them promising materials for gas storage and catalysis.[4,5] Applied synthetic approaches to high-surface area MOFs generally pursue *reticular* concepts whereby a rational consideration of the structural characteristics of inorganic and organic nodes results 20 'default' topologies.[6] The use of extended, rigid organic linkers allows the preparation of highly augmented, low-density materials with surface areas exceeding 7000 m^2/g.[7]

In recent years, the significance of polymorphism or framework isomerism of MOFs has been recognized.[8] To improve storage 25 capabilities or to understand the role of MOFs in shape/size selective catalysis and compare reaction rates, it is desirable to study toplogical isomers with identical framework compositions.
The combination of SBUs with square and triangular nodal topologies typically leads to two edge-transitive default 30 topologies that can be described by the RCSR symbols **tbo** and **pto**.[9] Examples of MOFs with **tbo** topology are HKUST-1,[10] PCN-6/6'[11] and MOF-399;[12] **pto**-networks, occur e.g. in MOF-14,[13] MOF-143/DUT-34[12,14] and MOF-388.[12] Here we report two polymorphic framework structures with the composition 35 [Cu$_3$(BTEB)$_2$(H$_2$O)$_3$] that allow the first direct comparison of topological pto- and tbo-isomers of MOFs that are composed of {Cu$_2$} SBUs with square nodal topology. In previous accounts the applied reaction conditions and a judicative choice of organic and inorganic SBUs, preferentially resulted in the selective formation 40 of compounds with either tbo or pto topology. To the best of our knowledge, true topological pto and tbo isomers for an identical pair of organic and {Cu$_2$} SBUs have not yet been reported. Our synthetic approach utilises the tritopic linker, 1,3,5-benzene-trisethynylbenzoic acid (BTEB) that stabilises highly augmented 45 Cu^{II} 'paddlewheel'-type MOFs whereby the **tbo** topology obtained gives rise to a significantly higher surface area than that of the corresponding **pto** isomer. The reaction between BTEB and Cu(NO$_3$)$_2$.3H$_2$O in DMF in the presence of 4,4'-bipyridine
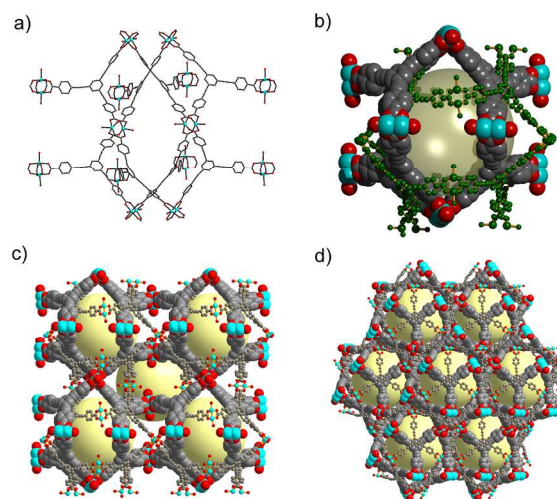

Fig. 1. a) Characteristic structural unit of the **pto**-network in **TCM-4'**; b) Interpenetrated **pto** motifs; c) and d) Packing diagram of the 2-fold interpenetrated **pto**-net with view in the crystallographic [110]- and [101]-directions; largest solvent-accessible void spaces are depicted as yellow spheres whereby the H-atoms and constitutional solvent molecules have been omitted for clarity; colour code Cu cyan, O red, C grey.

(bpy) at 85 °C produces the 2-fold interwoven **pto**-type topology 50 in **TCM-4'** which crystallises in the monoclinic space group *C*2/*c*. Slight modifications of the applied reaction conditions produce the closely related **pto**-type MOF **TCM-4** that crystallises in the body-centred cubic space group *Im*-3 which has previously been reported by us.[15]

55 In **TCM-4'**, each dinuclear {Cu$_2$} paddlewheel SBU binds to four BTEB residues and each BTEB ligand connects three dinuclear {Cu$_2$} complexes. This connectivity stabilises a (3,4)-net with augmented Pt$_3$O$_4$ topology in which triangular BTEB units substitute the 3-connected nodes and the {Cu$_2$} complexes 60 replace the 4-connected vertices. Fig. 1a highlights the characteristic structural units of the resulting **pto**-type network. The formation of the dual, interwoven framework structure is favoured by the co-existence of slightly condensed and more augmented structural units that interpenetrate each other (Fig. 65 1b). The observed dual assembly in which individual sub-nets are displaced from one another by (½, ½, ½) reinforces the augmented topology (Fig. 1c). The BTEB linkers are slightly bowed to facilitate the interweaving of the sub-nets (Fig. 1d) and engage in stabilising π-π interactions which involve the central 70 phenyl moieties. The **pto**-network topology stabilises

ChemComm Accepted Manuscript

exceptionally large cuboctahedral cavities that are also preserved in the 2-fold interwoven structure as shown in Fig. 1b.

It is important to note that 4,4'-bipyridine (bpy) is essential for the the formation of the here observed **pto**-type structure. However, one can only speculate on the role of this potential structural template; its size corresponds well with the observed 'intermolecular' distances between dinuclear {Cu$_2$} 'paddlewheel' units in the BTEB-stabilised **pto** network.[15] This matching spacial distance of N-donor atoms may influce the arrangement of the dinuclear {Cu$_2$} units during the crystallisation of **TCM-4'**. In the absence of 4,4'-bpy, or when the bipyridine is substituted by pyridine, **TCM-8** forms phase-pure in good yields under the reaction conditions detailed (ESI). The single crystal X-ray analysis reveals that **TCM-8** crystallises in a monoclinic space group $C2/m$. In contrast to **TCM-4'**, it is comprised of a network structure with the isomeric, edge-transitive, binodal (3,4) **tbo**-topology.

Fig. 2 shows the characteristic structural units in **TCM-8**. The **tbo** structure is characterized by larger cuboctahedral cavities that are surrounded by eight smaller octahedral cages. The latter cages adopt approx. T$_d$-symmetry and are comprised of four BTEB moieties that cover alternating, opposite-located triangular faces; the vertices of the octahedron are provided by six cis/90° coordinated {Cu$_2$} units with square nodal symmetry. Hence, this resulting structural motif closely relates to the comparable molecular {M$_6$L$_4$} cages (M = Pd^{II}, Pt^{II}; L= 2,4,6-tri(pyridine-4-yl)-1,3,5-triazine) developed by Fujita et al.[16a] The larger cuboctahedral cages in **TCM-8** analogously relate to molecular species formed between Cu^{II} paddlewheel complexes and ditopic 120°-linkers (i.e. isophthalate linkers).[16b] As for **TCM-4'**, **TCM-8** is two-fold interpenetrated and contains two symmetry-equivalent nets whose equivalent positions are displaced by (½, ½, ½) with respect to each other. Thus, the structural features of both of the compounds discussed here are directly comparable. The interpenetration in **TCM-8** results in an arrangement whereby the smaller octahedral cages of one net are now located within the larger cuboctahedral cavities of the second net to give a endohedral assembly of Platonic (octahedron) and Archimedean bodies (cuboctahedron).

It should be mentioned that the crystal structures of **TCM-4'** and **TCM-8** both adopt lower symmetry settings than other archetype {Cu$_2$}-based MOFs with **pto** and **tbo** topologies that typically crystallise in the Fm-3 and Pm-3 space groups. This feature is attributable to the observed structural flexibility of the acetylene-based BTEB ligand. This characteristic may also be an important factor for the encountered polymorphism. Both structure types, **pto** and **tbo** networks are defined by specific binding geometries that can be exemplified, as previously highlighted by Yaghi et al.,[12] by the dihedral angles between the plane of central phenyl ring of the BTEB ligand and the square nodal plane of the attached {Cu$_2$} SBUs. In the structures with ideal, high symmetry settings these angles are 55° for a **pto** network and 90° for a **tbo** network. Whilst preparative approaches using triangular and square {Cu$_2$} SBUs generally led to one of these default topologies, framework isomers or transition between the phases are not observed, as for many polyaromatic linkers a free rotation of the binding carboxylate moieties is often hampered by geometrical restraints. In many cases steric restraints between the H-atoms of the central and peripheral phenyl rings stabilize one particular conformation. The introduction of acetylene moieties into the ligand system partially alleviates these geometrical restraints and increases the structural flexibility to give structures with diverting dihedral angles between the planes of the central phenyl moiety and the {Cu$_2$} SBU; in **TCM-4'** the angle is $ca.$ 50° and in **TCM-8** it is 89°.

Both **TCM-4'** and **TCM-8** represent MOFs with highly augmented topologies that are characterised by solvent accessible void volumes of $ca.$ 78% and 84% of the cell volumes. Thermogravimetric analyses further underline these structural attributes and freshly prepared samples of **TCM-4'** and **TCM-8** undergo a weight loss of 63% and 72% between 30-120 °C due to the loss of constitutional solvent molecules. However, preliminary BET measurements demonstrate that both compounds only reveal a limited structural integrity when desolvated using conventional drying approaches. Due to the difficulty to achieve fully desolvated frameworks that maintain their characteristic **pto** and **tbo** topologies (ESI), theoretical calculations were carried out to characterise the potential surface
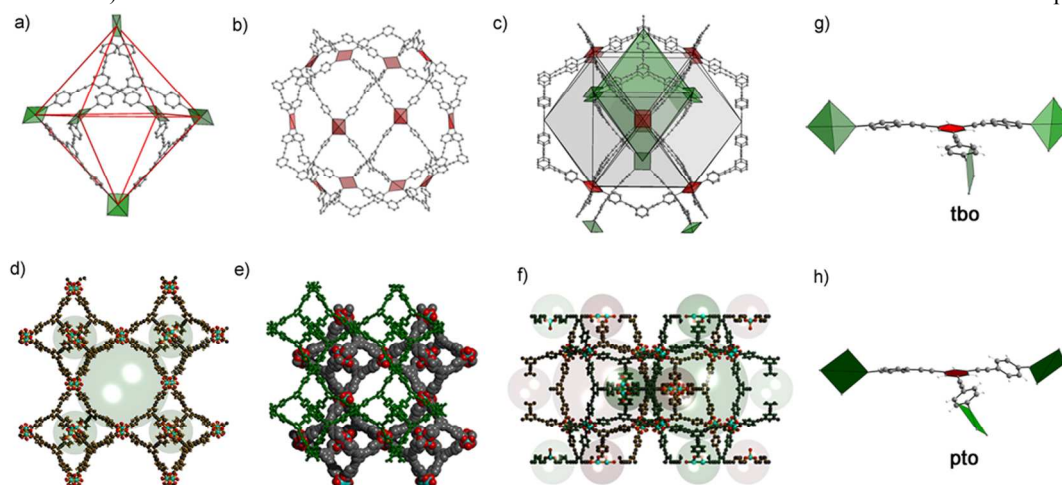

Fig.2. a) Representation of the octahedral {{Cu$_2$}$_6$(BTEB)$_4$} cage in **TCM-8**; b) and c) Representation of the cuboctahedral cavity and the interpenetration of octahedral and cuboctahedral cages in **TCM-8**, respectively; d) and e) Structure of **TCM-8**, approx. with view in the direction of the crystallographic [101]-direction (single framework d); dual framework e)). Representation of the cavities in the dual interpenetrated framework structure of **TCM-8** (cavities that arise from framework I shaded in green whilst those that arise from framework II are shaded in red); e) and f) Binding geometry of the BTEB ligand in **TCM-4'** (**pto**) and **TCM-8** (**tbo**); see $also$ $enlarged$ $Figures$ in the ESI.

areas and storage capabilities. The pore size distributions (PSD) were calculated using a method which determines the largest sphere that can be inserted into the structure without any overlap with framework atoms (Fig. 3, *inset*).[17] The open-framework

[5] structure of **TCM-8** is more complex than that found in **TCM-4'**, containing three distinct micropores of 12.3, 14.5 and 18.5 Å in diameter. The pore system of **TCM-4'** is characterized by single, defined pores with large cross-sectional diameters of 22 Å and smaller narrow windows of 9 Å. The accessible surface areas

[10] (Tab. 1) were found to be more than 40% higher in **TCM-8** than in **TCM-4'**. Simulated N_2 adsorption isotherms at 77 K are presented in Fig. 3. In agreement with the calculated surface areas and pore volumes, the maximum nitrogen capacity of **TCM-8** of 76 mmol/g is *ca.* 43% higher than that of **TCM-4'** (53 mmol/g).
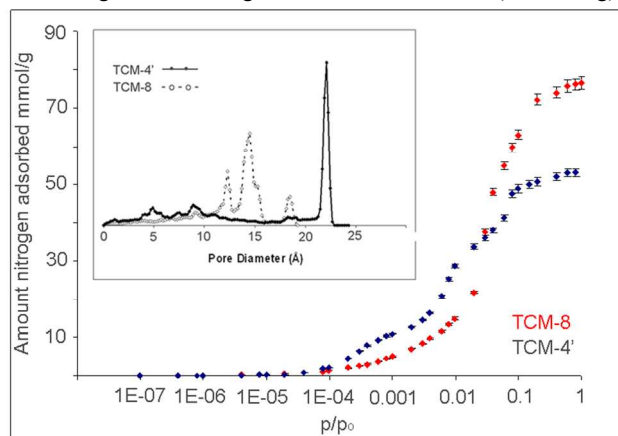

[15] **Fig. 3** Simulated N_2 adsorption isotherms for **TCM-4'** and **TCM-8**. *Inset*: Pore-size distributions.

Tab. 1 Solvent-accessible void volume, calculated accessible surface area and helium pore volume of **TCM-4'** and **TCM-8**.

[20]

Compound	Void Volume ($Å^3$, % of unit cell volume)	Accessible Surface Area (m^2/g)	He-pore vol. (cm^3/g @298 K)
TCM-4'	63340, 78.3%	3820	1.85
TCM-8	88500, 83.8%	5441	2.67

The two structures produce very different isotherm types. In the case of **TCM-4'**, several points of inflexion are apparent. These correspond to the localisation of N_2 molecules within the pore

[25] windows and, subsequently, near the BTEB linkers before finally filling the centre of the large cavity. **TCM-4'** is characterised by a Type IV isotherm, consistent with the mesoporous nature of the MOF. In the case of **TCM-8**, the low-pressure uptake is considerably reduced as a consequence of the significantly larger

[30] pore windows. Although three different cavity types are present in **TCM-8**, the pressure ranges at which these pores fill overlap, resulting in a smooth, well defined, Type I isotherm.

In summary, we describe the synthesis of highly augmented {Cu$_2$} 'paddlewheel'-based MOFs that are stabilized by BTEB

[35] linkers. The applied synthetic approaches that take advantage of 4,4'-bipyridine as topological modifier, result in the framework isomers of 2-fold interpenetrated, **pto-** and **tbo**-structures that are directly comparable. Calculations demonstrate that the potential pore volume, surface area and N_2 capacity of the **tbo**-structure,

[40] **TCM-8**, are substantially higher those of the **pto** counterpart.

Notes and references

[a] School of Chemistry & CRANN, University of Dublin, Trinity College, Dublin 2, Ireland. Tel: (+) 353-1-896-3495; E-mail: schmittw@tcd.ie
[45] *[b] Institute for Materials and Processes, School of Engineering, The University of Edinburgh, Mayfield Road, Edinburgh, EH9 3JL, UK.*

1   *Metal-organic frameworks-design and application* (Eds.: L. R. McGillivray), John Wiley & Sons, Inc. 2010.
2   *special issues* (a) *Chem. Rev.* 2012, **112**, issue 2; (b) *Chem. Soc. Rev.* 2009, **38**; c) A. K. Cheetham, C. N. R. Rao, *Science* 2007, **318**, 58.
3   (a) J. Yang, A. Sudik, C. Wolverton, D. J. Siegel, *Chem. Soc. Rev.* 2010, **39**, 656; (b) D. J. Collins, H. C. Zhou, *J. Mat. Chem.* 2007, **17**, 3154; (c) H. Furukawa, K. E. Cordova, M. O'Keeffe, O. M. Yaghi, *Science*, 2013, **341**, 6149; (d) M. Yoon, K. Suh, S. Natarajan, K. Kim, *Angew. Chem. Int. Ed.* 2012, **52**, 2688.
4   (a) W. Lin, *J. Solid State Chem*. 2005, **178**, 2486; (b) R.-Q. Zou, H. Sakurai, S. Han, R.-Q. Zhong, Q. Xu, *J. Am. Chem. Soc.* 2007, **129**, 8402; (c) S. Horike, M. Dincã, K. Tamaki, J. R. Long, *J. Am. Chem. Soc.* 2008, **130**, 5854; (d) Y. Liu , W. Xuan , Y. Cui, *Adv. Mater.* 2010, **22**, 4112.
5   (a) J. L. C. Rowsell, O. M. Yaghi, *Angew. Chem. Int. Ed.* 2005, **44**, 4670; (b) X. Lin, J. Jia, P. Hubberstey, M. Schröder, N.R. Champness, *CrystEngComm* 2007, **9**, 438; (c) M. Dinca, J. R. Long, *Angew. Chem. Int. Ed.* 2008, **47**, 6766; (d) R. E. Morris, P. S. Wheatley, *Angew. Chem. Int. Ed.* 2008, **47**, 4966; (e) X. S. Wang, S. Ma, D. Sun, S. Parkin, H. C. Zhou, *J. Am. Chem. Soc.* 2006, **128**, 16474.
6   O. M. Yaghi, M. O'Keeffe, N. W. Ockwig, H. K. Chae, M. Eddaoudi, J. Kim, *Nature* 2003, **423**, 705.
7   (a) H. Furukawa, N. Ko, Y. B. Go, N. Aratani, S. B. Choi, E. Choi, A. O. Yazaydin, R. Q. Snurr, M. O'Keeffe, J. Kim, O. M. Yaghi, *Science* 2010, **239**, 424; (b) D. Yuan, D. Zhao, D. Sun, H.-C. Zhou, *Angew. Chem. Int. Ed*. 2010, **49**, 5357; (c) O. K. Farha, A. O. Yazaydın, I. Eryazici, C. D. Malliakas, B. G. Hauser, M. G. Kanatzidis, S. T. Nguyen, R. Q. Snurr, J. T. Hupp, *Nat. Chem.* 2010, **2**, 944; (d) Y. Yan, X. Lin, S. Yang, A. J. Blake, A. Dailly, N. R. Champness, P. Hubberstey, M. Schröder, *Chem. Commun.* 2009, 1025.
8   (a) J. P. Zhang, X. C. Huang, X. M. Chen, *Chem. Soc. Rev.* 2009, **38**, 2385; (b) T. A. Makal, A. Yakovenko, H. C. Zhou, *J. Phys. Chem. Lett.*, 2011, **2**, 1682; (c) M. R. Kishan,. J. Tian, P. K. Thallapally, C. A. Fernandez, S. J. Dalgarno,. J. E. Warren,. B. P. McGrail, J. L. Atwood, *Chem. Commun.*, 2010, **46**, 538.
9   (a) O. Delgado-Friedrichs, M. O'Keeffe, O. M. Yaghi, *Phys. Chem. Chem. Phys.* 2007, **9**, 1035; (b) M. O'Keeffe, M. A. Peskov, S. J. Ramsden, O. M. Yaghi, *Acc. Chem. Res.* 2008, **41**, 1782.
10   S. S.-Y. Chui, S. M.-F. Lo, J. P. H. Charmant, A. G. Orpen, I. D. Williams, *Science* 1999, **283**, 1148.
11   (a) D. Sun, S. Ma, Y. Ke, D. J. Collins, H.-C. Zhou, *J. Am. Chem. Soc.* 2006, *128*, 3896; (b) S. Ma, D. Sun, M. Ambrogio, J. A. Fillinger, S. Parkin, H.-C. Zhou, *J. Am. Chem. Soc.* 2007, **129**, 1858.
12   H. Furukawa, Y. B. Go, N. Ko, Y. K. Park, F. J. Uribe-Romo, J. Kim, M. O'Keeffe, O. M. Yaghi, *Inorg. Chem*. 2011, **50**, 9147.
13   B. Chen, M. Eddaoudi, S. T. Hyde, M. O'Keeffe, O. M. Yaghi, *Science* 2001, **291**, 1021.
14   N. Klein, I. Senkovska, I. A. Baburin, R. Grünker, U. Stoeck, M. Schlichtenmayer, B. Streppel, U. Müller, S. Leoni, M. Hirscher, S. Kaskel, *Chem. Eur. J.* 2011, **17**, 13007.
15   N.-Y. Zhu, M. J. Lennox, G. Tobin, L. Goodman, T. Düren, W. Schmitt, *Chem. Eur. J.,* 2014, DOI: 10.1002/chem.201304856.
16   (a) M. Fujita, M. Tominaga, A. Hori, B. Therrien, *Acc. Chem. Res.* 2005, **38**, 371; (b) S. S.-Y. Cui, M.-F. Lo , J. P. H. Charmant, A. G. Orpen, I. D. Williams, *Science* 1999, **283**, 1148.
17   L. D. Gelb, K. E. Gubbins, *Langmuir* 1998, **14**, 2097.

Graphical Abstract:
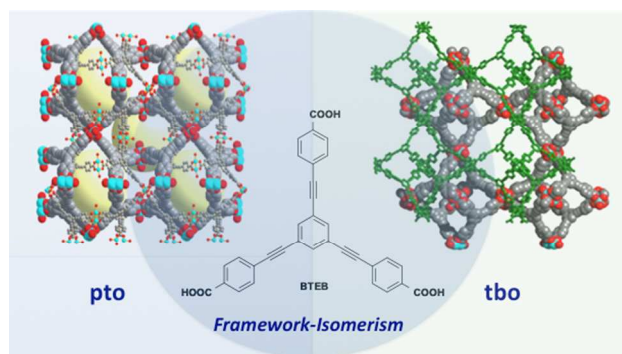
Abstract: The syntheses, calculated surface areas and N_2 uptakes of two highly augmented $\{Cu\}_2$ 'paddlewheel'-based MOFs provide a direct comparison of *tbo* or *pto* framework polymorphs.